

# Solar-neutrino oscillations and third-flavour admixture

P. Osland<sup>a,b</sup> and G. Vigdel<sup>a</sup>

<sup>a</sup>*Department of Physics, University of Bergen,  
Allégaten 55, N-5007 Bergen, Norway*

<sup>b</sup>*Theoretical Physics Division, CERN, CH-1211 Geneva 23, Switzerland*

## Abstract

With one  $\Delta m^2$  of the appropriate order of magnitude to solve the atmospheric neutrino problem, we study the resulting three-generation vacuum-oscillation fit to the solar neutrino flux. An explanation of the atmospheric neutrino composition in terms of pure  $\nu_\mu \rightarrow \nu_\tau$  oscillations is easily compatible with the well-known two-flavour oscillation solution for solar neutrinos. The allowed parameter region in the  $\sin^2(2\theta_{12})$ - $\Delta m^2$  plane changes little with increasing values of the mixing element  $U_{e3}$ , provided this is less than about 0.4. We find that the threefold maximal mixing is disfavoured.

# 1 Introduction

While neutrino-oscillation experiments tend to suffer from systematic errors that are difficult to estimate, there are at least two distinct neutrino problems that deserve serious consideration: the deficit of solar neutrinos and the atmospheric neutrino composition. The former has been around for many years. It started with the pioneering Homestake detector and later gained significance with the water-scattering and gallium experiments [1].

The latter anomaly is an inconsistency between the number of detected neutrinos of the muon family and those of the electron family, assumed to be generated by cosmic-ray hadrons impinging on the atmosphere. The ratio of ratios

$$R = \frac{(N_\mu/N_e)_{\text{observed}}}{(N_\mu/N_e)_{\text{predicted}}}, \quad (1)$$

where  $N_\mu$  is the number of  $\mu$ -like events and  $N_e$  the number of  $e$ -like events, should be, according to theory, close to 1, but is instead around  $\sim 0.6$  [2].

If one analyses the solar-neutrino deficit (a summary of the chlorine [3], gallium [4, 5] and water-scattering experiments [6, 7] is given in Table 1) in terms of two-flavour mixing, the vacuum-oscillation solution leads to a set of disconnected regions in the two-dimensional parameter space spanned by  $\sin^2(2\theta)$  and  $\Delta m^2$ , according to the  $\nu_e$  survival probability

$$P_{\nu_e \rightarrow \nu_e}(t) = 1 - \sin^2(2\theta) \sin^2\left(\frac{\Delta m^2 t}{4E}\right), \quad (2)$$

where  $\theta$  is the mixing angle,  $\Delta m^2$  the difference of the squared masses,  $t$  the time since creation and  $E$  the neutrino energy. The favoured region is  $\sin^2(2\theta) \simeq 0.8$ – $0.9$ , with  $\Delta m^2 \simeq 6 \times 10^{-11} \text{ eV}^2$ , but neighbouring regions that differ from  $\Delta m^2$  by  $n \times \delta m^2$  can yield comparable values of  $\chi^2$ , provided  $n$  is a small integer, and  $\delta m^2$  is of the order of  $1.4 \times 10^{-11} \text{ eV}^2$  (cf. Fig. 1a)<sup>1</sup>. The scale  $\delta m^2$  is given by the characteristics of the detectors, the neutrino energy (of the order of a MeV) and the distance  $R$  from the Sun to the Earth:  $\delta m^2 \simeq 4\pi E\hbar c/R$ .

The probability expression (2) and Fig. 1a show the ‘just so’ character of vacuum oscillations, the mass-squared difference has to be fine-tuned in relation to the Sun–Earth distance if this model shall solve the solar-neutrino problem [9]. (The allowed region in the upper part of Fig. 1a, where  $\Delta m^2 > 2 \times 10^{-10} \text{ eV}^2$ , is a new feature of the most recent data [10].)

With three flavours of neutrinos, one may consider the general three-flavour mixing, in which a state, which is of pure flavour  $\alpha$  ( $\alpha = e, \mu, \tau$ ) at  $t = 0$ , evolves as

$$\nu(t) = \sum_j U_{\alpha j} e^{-iE_j t} \nu_j, \quad (3)$$

---

<sup>1</sup>The MSW [8] interpretation of the data leads to values of  $\Delta m^2$  that are several orders of magnitude higher.

where the summation index  $j$  runs over mass states. We write the unitary mixing matrix as

$$U = \begin{bmatrix} U_{e1} & U_{e2} & U_{e3} \\ U_{\mu1} & U_{\mu2} & U_{\mu3} \\ U_{\tau1} & U_{\tau2} & U_{\tau3} \end{bmatrix}. \quad (4)$$

The full parameter space then consists of three angles (we ignore  $CP$ -violating effects) and two independent squared-mass differences (the energy can be approximated as  $E_j \simeq p + m_j^2/2E$ ). In particular, the survival probability of an electron neutrino takes the form

$$P_{\nu_e \rightarrow \nu_e}(t) = 1 - 4 \left[ U_{e1}^2 U_{e2}^2 \sin^2 \left( \frac{\Delta m_{21}^2 t}{4E} \right) + U_{e1}^2 U_{e3}^2 \sin^2 \left( \frac{\Delta m_{31}^2 t}{4E} \right) + U_{e2}^2 U_{e3}^2 \sin^2 \left( \frac{\Delta m_{32}^2 t}{4E} \right) \right], \quad (5)$$

where  $\Delta m_{ij}^2 = m_i^2 - m_j^2$ . Unitarity and data on other phenomena, in particular on the atmospheric neutrino flux, lead to constraints on these parameters.

We denote the mass states  $\nu_1$ ,  $\nu_2$  and  $\nu_3$ , according to their intrinsic mass ratio: their respective mass eigenvalues will be sorted as  $m_1 < m_2 < m_3$ . For the mixing matrix we use the form advocated for quarks by the Particle Data Group [11]<sup>2</sup>:

$$U = U_{\mu\tau}(\theta_{23})U_{e\tau}(\theta_{13})U_{e\mu}(\theta_{12}) = \begin{bmatrix} c_{12} c_{13} & s_{12} c_{13} & s_{13} \\ -c_{12} s_{13} s_{23} - s_{12} c_{23} & -s_{12} s_{13} s_{23} + c_{12} c_{23} & c_{13} s_{23} \\ -c_{12} s_{13} c_{23} + s_{12} s_{23} & -s_{12} s_{13} c_{23} - c_{12} s_{23} & c_{13} c_{23} \end{bmatrix}, \quad (6)$$

where  $c_{12} = \cos \theta_{12}$ ,  $c_{13} = \cos \theta_{13}$ , etc., and the mixing angles  $\theta_{12}$ ,  $\theta_{13}$  and  $\theta_{23}$  are in the interval  $[0, \pi/2]$ .

## 2 Three-parameter accommodation of the solar neutrino flux

A three-flavour analysis of the solar-neutrino oscillations will restrict the allowed values of the elements in the mixing matrix. Because of unitarity, the solar electron-neutrino survival probability can always be expressed in terms of only *two* mixing angles, here taken to be  $\theta_{12}$  and  $\theta_{13}$ . We shall assume that the dominant mixing (represented in Fig. 1a) is a mixing between the first two families, and ask (i) ‘How will the goodness of fit depend on  $U_{e3}$ ’ and (ii) ‘How will the allowed regions of Fig. 1a change as one increases the strength of this mixing?’

Before we address these questions, we want to introduce some further restrictions on the neutrino parameters: we reserve one  $\Delta m^2$  for the vacuum-oscillation

---

<sup>2</sup>There are nine structurally different ways to express the mixing matrix in terms of mixing angles. A discussion of the parametrization of flavour mixing in the quark sector is presented in [12], where also  $CP$  violation is included.

solution of the solar-neutrino problem,  $\Delta m_{21}^2 \sim 10^{-11} \text{ eV}^2$ . The suppression of atmospheric muon neutrinos relative to electron neutrinos suggests that also  $\nu_\mu$  oscillates into some other flavour of neutrinos, but (since the ratio  $t/E$  relevant to atmospheric neutrinos is orders of magnitudes smaller than that for solar neutrinos) with a mass-squared difference that is many orders of magnitude larger than is required to explain the solar-neutrino deficit. It is therefore natural to assume that other squared-mass differences are much larger:

$$\Delta m_{21}^2 \sim 10^{-11} \text{ eV}^2 \ll \Delta m_{32}^2 \lesssim \Delta m_{31}^2, \quad (7)$$

such that when Eq. (5) is applied to the case of solar neutrinos, the last two terms can be represented by their average values:

$$P_{\nu_e \rightarrow \nu_e}^{\text{sun}}(t) = 1 - \sin^2(2\theta_{12}) \cos^4 \theta_{13} \sin^2 \left( \frac{\Delta m_{21}^2 t}{4E} \right) - \frac{1}{2} \sin^2(2\theta_{13}). \quad (8)$$

Here, the last term represents a non-zero component of the  $\nu_3$  mass state in the electron-neutrino state, and vanishes with  $|U_{e3}|^2$ . For  $\theta_{13} = 0$  we get the familiar two-family mixing of Eq. (2).

While a simultaneous fit to both solar- and atmospheric-neutrino fluxes also would involve the angle  $\theta_{23}$  as well as two mass-squared differences, under the assumption (7) the above formula (8) provides a three-parameter accommodation of the solar flux.

We show in Fig. 1b the results of two-parameter fits to the solar-neutrino data. (The high region in  $\Delta m^2$ , cf. Fig. 1a, is not displayed here.) In our calculations we use the solar-neutrino flux as given by the 1998 Standard Solar Model (SSM) by Bahcall, Basu and Pinsonneault [10], and for the detection rates the values given in Table 1. The second mixing angle,  $\theta_{13}$ , is held fixed at different values, and the fit is performed in the variables  $\sin^2(2\theta_{12})$  and  $\Delta m_{21}^2$ . It is seen that regions that are separated in the two-family case, can be smoothed out to one big region when the more general case of three flavours is considered. However, there is a slight worsening of the quality of the fit as the coupling to the third state is increased. For  $\sin \theta_{13} = 0.0, 0.2, \text{ and } 0.4$ , the values of  $\chi_{\text{min}}^2$  are 3.6, 4.2 and 5.6, respectively. For two degrees of freedom, 4 experiments (SAGE and GALLEX are combined) minus 2 parameters, the probability of getting  $\chi^2$  larger than those values by chance, are 17, 12 and 6%, respectively. None of these is particularly good, but they are not excluded.

Since there is some uncertainty associated with the important boron flux [10], we have checked how the fit changes under 10% rescalings of the  ${}^8\text{B}$  flux. In Table 2 we show the resulting  $\chi_{\text{min}}^2$  and goodness of fit for three different fractions of the SSM boron flux (keeping the other components of the flux fixed), for two different values of  $U_{e3}$ . For the lowest of these fractions, the goodness of fit is appreciably better than for the standard  ${}^8\text{B}$ -flux. It is also seen that, for the lowest of our tabulated boron flux values, the fit deteriorates less when  $\sin \theta_{13}$  is non-zero.

A different representation, for several values of  $\sin\theta_{13}$ , is given in Fig. 2, including also the higher- $\Delta m^2$  region. As  $\sin\theta_{13}$  increases, the allowed regions get broader, but also the fit gets poorer.

It has been argued that the data suggest ‘maximal mixing’ [13]. In our variables, maximal mixing corresponds to  $\sin^2(2\theta_{12}) = 1$  and  $\sin\theta_{13} = 1/\sqrt{3} \simeq 0.58$ . We find that the fit gets rather poor for such parameters, with  $\chi_{\min}^2 = 11$ .

### 3 Long-baseline experiments

The future long-baseline experiments [14] will provide new restrictions on these mixing elements. For example, if we assume that a long-baseline experiment is such that oscillations other than those involving

$$\Delta M^2 \equiv \Delta m_{31}^2 \simeq \Delta m_{32}^2 \quad (9)$$

can be neglected, then the condition (7) leads to the following transition probabilities:

$$P_{\nu_\mu \rightarrow \nu_e}^{\text{L.B.}}(t) = \sin^2\theta_{23} \sin^2(2\theta_{13}) \sin^2\left(\frac{\Delta M^2 t}{4E}\right), \quad (10)$$

$$P_{\nu_\mu \rightarrow \nu_\tau}^{\text{L.B.}}(t) = \cos^4\theta_{13} \sin^2(2\theta_{23}) \sin^2\left(\frac{\Delta M^2 t}{4E}\right), \quad (11)$$

and the survival probability:

$$P_{\nu_e \rightarrow \nu_e}^{\text{L.B.}}(t) = 1 - \sin^2(2\theta_{13}) \sin^2\left(\frac{\Delta M^2 t}{4E}\right). \quad (12)$$

Note that the coefficient in Eq. (10) can be written as  $4|U_{e3}|^2|U_{\mu3}|^2$ . The  $\nu_\mu \rightarrow \nu_e$  transition can thus be given a simple physical interpretation, valid for small values of the mixing angle  $\theta_{13}$ . When  $\Delta m_{21}^2 t/E \ll 1$ , the transition can be interpreted as an ‘indirect’ transition, involving the admixtures of  $\nu_3$  as given by  $\theta_{13}$  and  $\theta_{23}$ . This is different from the case of  $\Delta m_{21}^2 t/E \simeq 1$ , where the ‘direct’ transition  $\nu_e \rightarrow \nu_\mu$  is effective via the states  $\nu_1$  and  $\nu_2$ .

The atmospheric-neutrino data are usually explained in terms of  $\nu_\mu \rightarrow \nu_e$  or  $\nu_\mu \rightarrow \nu_\tau$  oscillations with a large amplitude [15, 16]. When applying Eq. (8) to explain the solar-neutrino deficit, the transition  $\nu_\mu \rightarrow \nu_\tau$  is preferable for the atmospheric neutrinos, because it allows for a small or vanishing value of  $\theta_{13}$ , which gives the best fit of the observed solar neutrino rate. An early three-flavour analysis (not including data from Super-Kamiokande) gave for the best fit a value for  $|U_{e3}|^2$  (or  $\sin^2\theta_{13}$ ) in the range 0.06–0.14 [17]. More recent studies (including Super-Kamiokande data) prefer values for  $\sin\theta_{13}$  of 0.1 [15] and  $< 0.1$  [16]. As we have seen, these low values of  $\sin\theta_{13}$  also lead to acceptable fits to the solar-neutrino data, with  $\chi_{\min}^2 = 3.6$ –5.6.

In the long-baseline experiments [14, 18], neutrinos from either an accelerator or a reactor will be counted after travelling a ‘long’ distance, from 1 km (for CHOOZ) to 730 km (for the MINOS experiment). In fact, the recent data from

the CHOOZ experiment, where the survival probability  $\bar{\nu}_e \rightarrow \bar{\nu}_e$  is measured, does not exclude any of the cases studied in Fig. 2, provided  $\Delta M^2 < 9 \times 10^{-4} \text{ eV}^2$ . Indeed, no evidence for oscillations was found for  $\Delta M^2 > 2 \times 10^{-2} \text{ eV}^2$  and  $\sin^2(2\theta_{13}) > 0.18$ . This means that  $\sin \theta_{13}$  has to be either small ( $< 0.22$ ) or quite big ( $> 0.98$ ) (or  $\Delta M^2 < 2 \times 10^{-2} \text{ eV}^2$ ). With the large-angle solution, Eq (8) gives a poor fit to the solar-neutrino data, this alternative should therefore be disregarded. The remaining low-angle solution is also preferred in the analysis of the atmospheric-neutrino data [15]. In this case (with  $\Delta M^2 > 2 \times 10^{-2} \text{ eV}^2$ ) the lower two boxes of Fig. 2 would be excluded. The Bugey reactor experiment [19], which is less sensitive, excludes  $\Delta M^2$  down to about  $3 \times 10^{-2} \text{ eV}^2$  for  $\sin \theta_{13} > 0.16$ , consistent with CHOOZ.

A measurement of a non-zero value for  $P_{\nu_\mu \rightarrow \nu_e}$  will imply a non-zero value for  $\theta_{13}$ . Such information, which would be a major result from the planned long-baseline experiments, combined with Eq. (8), can help us to further restrict the allowed parameter space relevant to the solar neutrinos.

We note that, for  $\nu_e \leftrightarrow \nu_\mu$  oscillations, the K2K experiment [20] will have a sensitivity of  $\sin^2(2\theta) > 0.1$  and the MINOS experiment could probe values as low as  $\sin^2(2\theta) = 0.01$ . In our parametrization, this means that they would be sensitive to values of  $\sin \theta_{13}$  as low as 0.16 and 0.05. If this mixing element should turn out to be significantly larger, the vacuum-oscillation solution to the solar-neutrino problem would have serious difficulties.

## 4 Concluding remarks

The data from the solar-neutrino detectors can very well be reconciled with the atmospheric-neutrino data. If we assume that the solution of the latter anomaly is the  $\nu_\mu \rightarrow \nu_\tau$  transition (which is induced by the direct mixing  $\theta_{23}$  and gives the best fit), then the vacuum-oscillation solution for the atmospheric and the solar-neutrino problems can be regarded as two separate two-generation oscillations. Even if the transition  $\nu_\mu \rightarrow \nu_e$ , which for  $\Delta m_{21}^2 L/E \ll 1$  is induced by the two-step process of  $\nu_e \nu_\tau$  and  $\nu_\mu \nu_\tau$  mixing (with angles  $\theta_{13}$  and  $\theta_{23}$ , respectively) should turn out to take place, the rate has to be quite large before it can severely alter the fit of the vacuum-oscillation solution to the solar-neutrino problem.

When the  $\nu_e \nu_\tau$  mixing angle  $\theta_{13}$  is increased from zero, the allowed ranges of  $\Delta m_{21}^2$  merge to a wider one, but beyond  $\sin \theta_{13} \simeq 0.5$ , which is well within the sensitivity that will be reached by the K2K experiment, the fit deteriorates rapidly.

## References

- [1] *Solar Neutrinos: The First 30 Years*, edited by: J. N. Bahcall et al. (Addison Wesley, New York, 1994);  
J. N. Bahcall, Phys. Lett. **B 338**, 276 (1994).
- [2] Y. Fukuda et al. (Super-Kamiokande Collaboration), ICRR-411-98-7 (1998),  
hep-ex/9803006 and hep-ex/9805006.
- [3] B. T. Cleveland, Nucl. Phys. (Proc. Suppl.) **B 38**, 47 (1995);  
K. Lande et al., in *Neutrino '96*, Proceedings of the 17th International Conference on Neutrino Physics and Astrophysics, Helsinki, 1996, edited by K. Huitu, K. Enqvist and J. Maalampi (World Scientific, Singapore, 1997).
- [4] P. Anselmann et al., Phys. Lett. **B 342**, 440 (1995);  
W. Hampel et al., Phys. Lett. **B 388**, 384 (1996).
- [5] J. N. Abdurashitov et al., Phys. Lett. **B 328**, 234 (1994). V. Gavrin et al.,  
in *Neutrino '96*, *op. cit.*
- [6] Y. Fukuda et al., Phys. Rev. Lett. **77**, 1683 (1996).
- [7] Y. Fukuda et al., hep-ex/9805021, submitted to Phys. Rev. Lett. See also  
Y. Itoh (contains S.K. data until 20 October 1997)  
[http://www-sk.icrr.u-tokyo.ac.jp/doc/sk/pub/pub\\_sk.html](http://www-sk.icrr.u-tokyo.ac.jp/doc/sk/pub/pub_sk.html)
- [8] S. P. Mikheyev and A. Yu. Smirnov, Yad. Fiz. **42**, 1441 (1985) [Sov. J. Nucl.  
Phys. **42**, 913 (1985)], Nuovo Cimento **9C**, 17 (1986);  
L. Wolfenstein, Phys. Rev. **D 17**, 2369 (1978), *ibid.* **20**, 2634 (1979).
- [9] V. Barger, R. J. N. Phillips and K. Whisnant, Phys. Rev. **D 24**, 538 (1981);  
S. L. Glashow and L. M. Krauss, Phys. Lett. **190 B**, 199 (1987).
- [10] J. N. Bahcall, S. Basu and M. H. Pinsonneault, astro-ph/9805135.
- [11] Particle Data Group (R. M. Barnett et al.), Phys. Rev. **D 54**, 1 (1996).
- [12] H. Fritzsch and Z.-z. Xing, Phys. Rev. **D 57**, 594 (1998); A. Rasin,  
hep-ph/9708216.
- [13] P. F. Harrison and W.G. Scott, Phys. Lett. **B333**, 471 (1994); P. F. Harrison,  
D. H. Perkins and W. G. Scott, Phys. Lett. **B349**, 137 (1995), *ibid.* **B374**,  
111 (1996) and **B396**, 186 (1997).
- [14] For a short description of some of these experiments, see *Neutrino '96*, *op. cit.*
- [15] O. Yasuda, hep-ph/9804400.
- [16] T. Teshima and T. Sakai, preprint CU-TP/98-05, hep-ph/9805386.

- [17] S. M. Bilenky, C. Giunti and C. W. Kim, *Astropart. Phys.* **4**, 241 (1996), hep-ph/9505301.
- [18] M. Apollonio et al. (CHOOZ Collaboration), *Phys. Lett.* **B 420**, 397 (1998).
- [19] B. Achkar et al., *Nucl. Phys.* **B 434**, 503 (1995).
- [20] Y. Oyama, talk at YITP Workshop on Flavour Physics, Kyoto, January 1998, hep-ex/9803014.

Experiment	Counting rate	SSM [10]	Counted/SSM
Homestake [3]	$2.54 \pm 0.14 \pm 0.14$	$7.7_{-1.0}^{+1.2}$	$0.330 \pm 0.026$
GALLEX [4]	$69.7 \pm 6.7_{-4.5}^{+3.9}$	$129_{-6}^{+8}$	$0.540_{-0.063}^{+0.060}$
SAGE [5]	$72_{-10-7}^{+12+5}$	$129_{-6}^{+8}$	$0.558_{-0.095}^{+0.100}$
Kamiokande [6]	$2.80 \pm 0.19 \pm 0.33$	$5.15_{-0.72}^{+0.98}$	$0.544 \pm 0.074$
Super-Kamiokande [7]	$2.42 \pm 0.06_{-0.07}^{+0.10}$	$5.15_{-0.72}^{+0.98}$	$0.470_{-0.017}^{+0.023}$

Table 1: Solar neutrino fluxes. Measured and SSM-predicted event rates are for the radio-chemical detectors measured in units of SNU (1 event per second per  $10^{36}$  target atoms). For the scattering detectors (the last two entries) the fluxes are in units of  $10^6 \text{ cm}^{-2} \text{ s}^{-1}$ . In the ratio of the observed to the predicted values, only experimental uncertainties are included.

	$\sin \theta_{13} = 0.0$			$\sin \theta_{13} = 0.3$		
	$f_B = 0.9$	$f_B = 1.0$	$f_B = 1.1$	$f_B = 0.9$	$f_B = 1.0$	$f_B = 1.1$
$\chi_{\min}^2$	2.0	3.6	5.8	2.9	4.8	7.2
$P(\%)$	38	17	5.5	23	9	3

Table 2: Best fits for different fractions,  $f_B$ , of the SSM  ${}^8\text{B}$  flux, for two different values of  $\sin \theta_{13} = U_{e3}$ . The lowest row gives the goodness of fit.

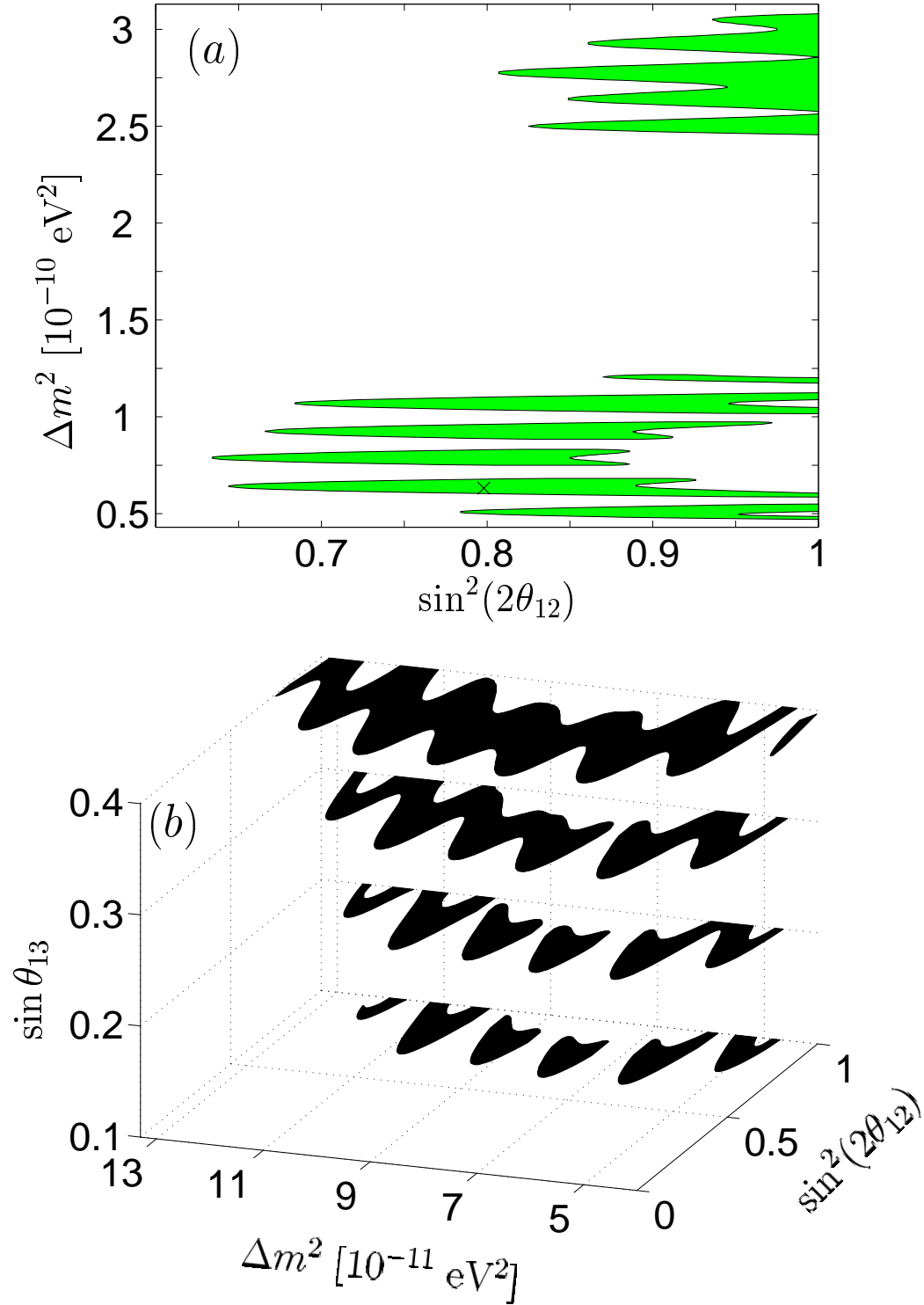


Figure 1: Allowed parameter space within 95% C.L. The upper figure illustrates the two-generation case, the cross marks the position of  $\chi^2_{\min}$ . The lower figure shows (under the assumption leading to Eq. (8)) the dependence on the mixing element  $U_{e3} = \sin \theta_{13}$ , which increases in steps of 0.1 from 0.1 to 0.4. The regions merge as the third mass state  $\nu_3$  gets more involved in the mixing.

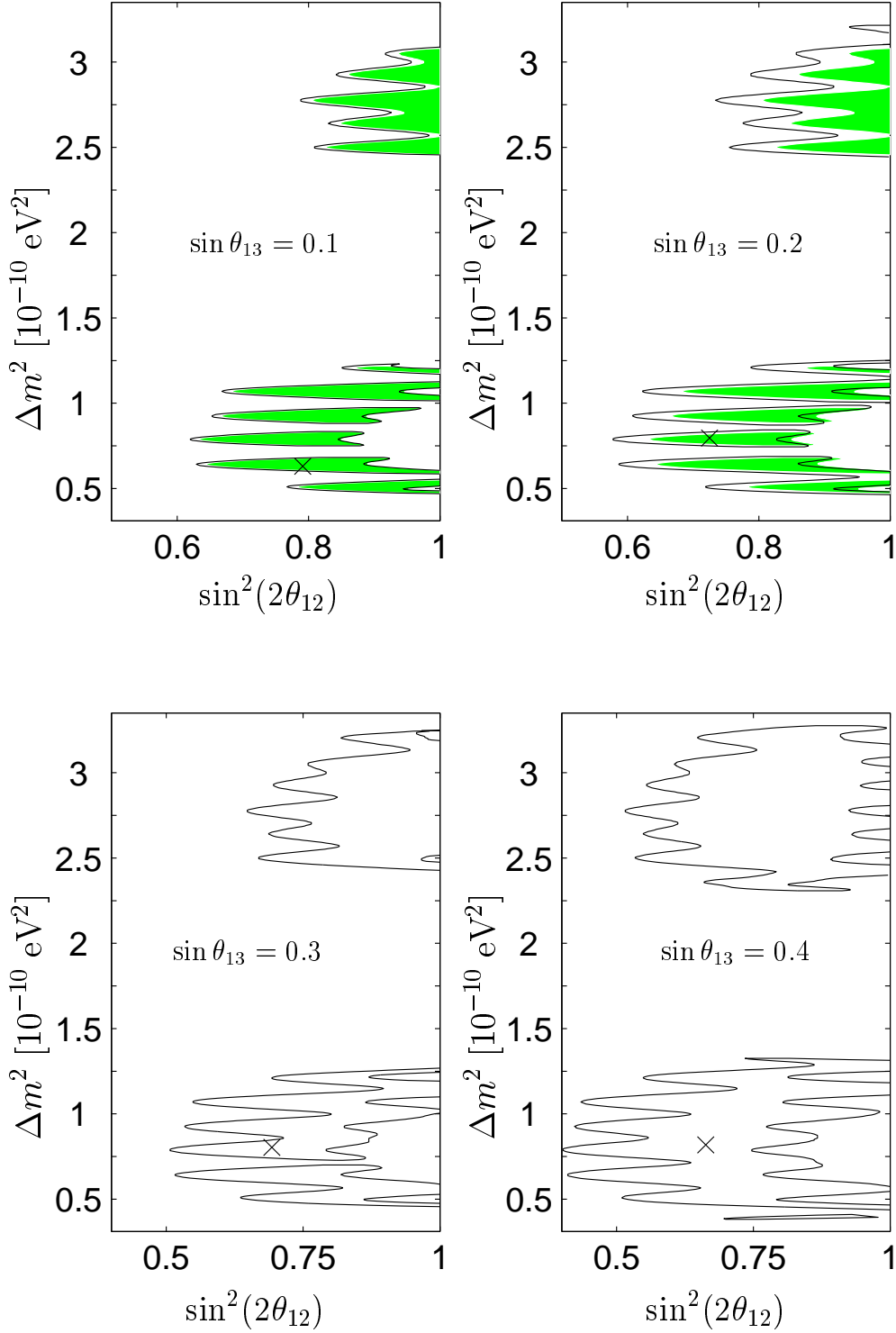


Figure 2: Allowed parameter space within 95% C.L. for  $\Delta M^2 \gg \Delta m^2$ , for different values of  $U_{e3}$  ( $= \sin \theta_{13}$ ). In the two upper boxes, the allowed regions for the two-generation oscillation (Fig. 1a) are also shown, as shaded areas. Note different horizontal scales. The crosses show the best-fit point.